

Poly(lactide-co-glycolide) / Clay nanocomposites: Effect of gamma irradiation

Manpreet Kaur¹, Surinder Singh¹, Rajeev Mehta²

¹Department of Physics, ²Department of Chemical Engineering

¹Guru Nanak Dev University, Amritsar-143005

²Thapar University, Patiala-147004

Email: manpreet984@gmail.com

Received 27 January 2017, received in revised form 15 February 2017, accepted 22 February 2017

Abstract: Gamma irradiation effect on poly(lactide-co-glycolide) PLGA and PLGA/organically modified montmorillonite clay (Cloisite® 30B) nanocomposites has been studied. The nanocomposites were successfully prepared by ultrasonication method and their morphological, optical and structural properties were characterized by scanning electron microscopy (SEM), X-ray diffraction (XRD), Fourier transform infrared (FTIR) and UV-Visible spectroscopic techniques respectively. Neat PLGA samples as well as those containing Cloisite® 30B were subjected to a gamma irradiation and a comparative study of changes induced in the nanocomposite structures and other properties was carried out. Results showed that neat PLGA is degraded by gamma irradiation to greater extent while PLGA/Clay nanocomposites are comparatively less affected. The morphological defects, after gamma radiation, were more pronounced in PLGA samples as compared to the PLGA/Clay nanocomposites samples.

Keywords: PLGA, Cloisite® 30B, nanocomposites, gamma irradiation.

1. INTRODUCTION

Sterilization by ionizing radiations is considered to be a useful technique to produce sterile drug-polymer-matrices for clinical uses[1]. Biodegradable polymer-based drug delivery systems are widely used to control the drug release [2-5]. Poly(lactide-co-glycolide) (PLGA) is the one of the synthetic biodegradable polymers which has many applications in biomedical and pharmaceutical fields [6]. It has been approved for controlled drug delivery use by the Food and Drug Administration, USA because it contains lactide and glycolide copolymer, which degrades according to their mole fraction and produce biocompatible and toxicologically safe products which are further eliminated by the normal metabolic pathways [7]. It provides many other numerous advantages in tissue engineering area also [8-10].

In order to improve the properties of degradable polymers, polymer nanocomposites have been prepared. The admixture of polymer and organically modified montmorillonite clay (OMMT) produces exfoliated or intercalated nanocomposites, which depend upon various characteristics of polymer and nanoclay used including the nature of the polymer as well as the type and the size of the organic modifiers on the silicate surface [11]. Ultrasonication method has been used to prepare

polymer/clay nanocomposites, to intercalate polymer chains into the silicate galleries or even results in exfoliation. Ultrasonication is an effective and convenient technique in which ultrasonic waves are used to cause the nanoscale dispersion of clay in polymer matrix [12-13]. The organically modified nanoclay (lateral dimensions varying from 100 nm to 150 nm) contain quaternary ammonium ions between clay platelets. The clay platelets are about 1nm thick and the inter-platelets distance is about 2-3 nm. The hydroxyl group on quaternary ammonium provides better binding energy of the organically modified nanoclay with the polymer containing ester linkages [14]. Dispersion of the clay platelets in polymer matrix results in a significant improvement in its yield stress, tensile strength, optical properties, gas barrier properties and that too at very low loading levels [15-16].

Several authors [17-20] have examined the influence of γ -irradiation on the degradation of PLGA, poly(lactic acid) (PLA) and poly(glycolic acid) (PGA) and some other polyester. Biodegradation of PLGA nanocomposites is known to be retarded with increasing dose due to the introduction of crosslinking during irradiation. Upon irradiation with γ -rays, PLGA undergoes structural changes, such as scission and crosslinking which in turn influences the drug carrier properties of degradable polymer [21]. These processes depend upon several factors, including the chemical structure of the polymer, rate and amount of dosage, and the environment of the material during irradiation [22]. γ -rays are easier to control, secure, reliable and provide a fast process. The biocompatibility, non-toxicity and non-inflammatory properties have been found in γ -irradiated PLGA which have been frequently used in bone repair applications [23-26]. γ -irradiation of biodegradable polymer is also an effective method for the exfoliation of clay platelets in the polymer matrix [27-29]. Although recent research suggest that the use of γ -irradiation on biodegradable polymer remains the only acceptable method, because γ -irradiation penetrates into the material, breaks the polymer chains and creates free radicals in polymer matrix by chain scission [30-32]. These free radicals may also recombine with one another to create inter chain cross-linking. These free radicals are responsible for the structural and chemical modifications through processes such as chain scission,

intermolecular cross linking, creation of unsaturated bonds, formation of volatile fragments and creation of carbonaceous clusters [33-36].

In the present study, it has been shown that PLGA nanocomposites can extend the properties (and potential applications) of the biodegradable polymer by adjustment of the nanoclay content. The present study investigates the effect of γ -irradiation on PLGA and its nanocomposites with various irradiation doses by X-ray Diffraction (XRD), Scanning Electron Microscopy (SEM), Fourier Transform Infrared (FTIR) and UV-Visible Spectroscopy. The influence of organically modified nanoclay (Cloisite[®] 30B) on the durability of the nanocomposite samples is also reported. It has been found that the gamma irradiation improves the physico-chemical properties of PLGA nanocomposites without causing significant degradation.

2. EXPERIMENTAL DETAILS

2.1 Materials and preparation of PLGA/Cloisite[®] 30B nanocomposites

PLGA (50:50) pellets (density 1.33g/cm³) were purchased from Lakeshore Biomaterials (USA). PLGA was prepared in a film form by the solvent casting method by dissolving it in dichloromethane (DCM). To avoid the formation of air bubbles, the resulting solution over glass plate was initially dried slowly at room temperature for two days and after that it was placed in an oven at 40°C for 7 days to remove the remaining solvent, leaving behind dried polymer film.

This procedure of removing the solvent at a very slow rate helps in preventing void development in the dried film. The PLGA/Clay nanocomposites were prepared by dissolving PLGA in DCM solvent. Organically modified montmorillonite (OMMT) powder purchased from Southern Clay Products was dispersed into this solution in different amounts (1wt%, 3wt% and 5wt%) by means of sonication using ultrasonic probe (Ultrasonic processor LABSONIC[®] Sartorius) for 15 min. Ultrasonication technique has been proven to yield homogenous dispersion of clay at a nano level in polymer matrix. The PLGA dissolved into the dispersion containing nanoclay was cast on a glass sheet and dried for 48 h at room temperature and further in an oven at 40°C for a week (same as for pure PLGA films), to obtain films of rectangular shape. The average thickness of the prepared films was about 33 μ m.

2.2 Gamma Irradiation

All the samples (PLGA and PLGA/Cloisite[®] 30B nanocomposites) were subjected to a series of radiation doses of 5 kGy, 10 kGy, 15 kGy, 25 kGy and 50 kGy using ⁶⁰Co source of gamma radiation (Gamma Chamber-1200) at Inter University Accelerator Centre (IUAC), New Delhi, India. These samples were irradiated for different time intervals to achieve the desired overall dose. γ -rays emitted by ⁶⁰Co have mean energy of 1.25 MeV and the dose rate in the irradiator was

7.5 kGy/h.

2.3 Characterization

The UV-VIS absorption spectra of the PLGA and its nanocomposites samples were recorded on a SHIMAZU UV-Visible Spectrophotometer over the range of 200–900 nm. The results of chemical modification due to γ -irradiation were monitored by FTIR spectroscopy. FTIR spectra of the samples were recorded using the NEXUS-670, FTIR spectrometer before and after irradiation, at different absorbed doses. Cloisite[®] 30B powder was ground together with dried KBr and compressed at high pressure into a disc. Spectra of this KBr disc, pure PLGA film and its nanocomposites films sample were recorded in transmission with 4 cm⁻¹ resolution mode in the 4000-500 cm⁻¹ region. The amorphous nature of these samples was confirmed by XRD using XRD-7000 SHIMADZU X-ray diffractometer with Cu K α radiation of wavelength $\lambda = 1.54 \text{ \AA}$ before and after irradiation for different γ -doses. The Bragg angle 2θ was kept in the range from 4° to 50° with a scanning speed of 2°/min. The surface morphology was observed with FEI, quanta 200F electron microscope (SEM) which was operated at accelerating voltage of 5KV. All the film samples were coated with a thin gold layer by means (SCD-005, sputter coated) gold sputter apparatus.

3. RESULTS AND DISCUSSION

3.1 UV-Visible analysis

Figures 1-4 show the changes in the absorption spectra of PLGA and PLGA/Clay nanocomposites upon γ exposure in the dose range of 0–50 kGy. It can be seen that the optical absorption edge is not sharply defined, thus clearly indicating the amorphous nature of the PLGA and PLGA/Clay nanocomposites film samples. From the absorption spectra, the indirect band gap, $(\alpha hv)^{1/2}$ was plotted as a function of photon energy (hv). The optical band gap is determined using following equation (Tauc's relation) [37].

$$\alpha(hv) = B[hv - E_g]^n / hv$$

where α is the absorption coefficient, hv is the photon energy, and E_g is the value of the optical energy gap. The values of indirect band gap (E_g) for pristine and gamma irradiated samples were determined by extrapolation of the straight part of the Tauc's plot (Fig. 5-8) and measuring the intercept value in hv axis are enlisted in Tables 1 and 2.

Sterilization by γ -radiation is known to cause chain scission in PLGA polymer [38-39]. At doses of 10 kGy γ -radiations, band gap decreases which indicate that chain scission occurred, which produced free radicals and caused deterioration of polymer chains. But at higher doses up to 50 kGy there was a small increase in optical band gap energy (Table 1). This may be attributed to the fact that, for gamma irradiation upto 50 kGy, recombination of free radicals or intermolecular cross-linking takes place within the polymer. It is evident that the free radicals

which are produced by ionizing radiations are then free to react with one another or initiate further reactions among the polymeric chains, thus giving rise to increased optical band gap energy of PLGA [40]. The absorbance difference of pristine and

irradiated polymer indicates that gamma irradiation enhances the UV absorbance and leads to formation of new chemical species as a result of energy transfer by the incidence of gamma rays.

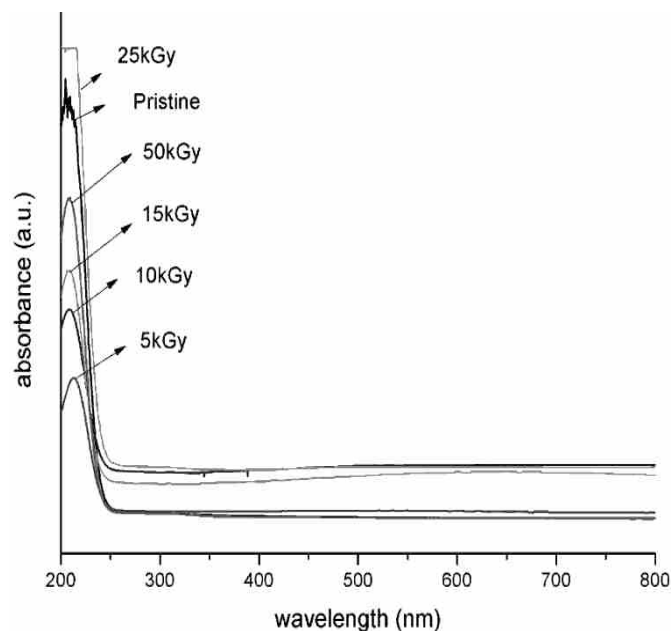


Fig.1. UV-Vis spectra of pristine and gamma irradiated PLGA samples

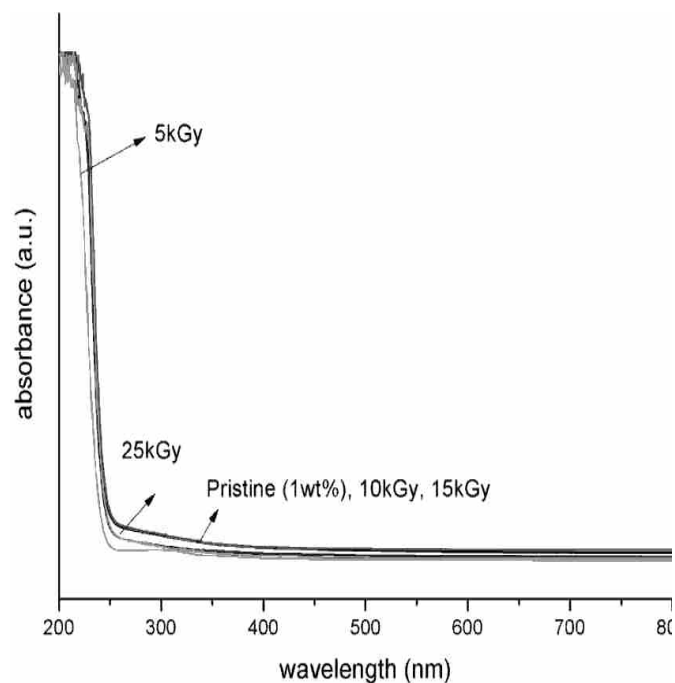


Fig.2. UV-Vis spectra of pristine and gamma irradiated PLGA nanocomposites samples containing 1wt% clay content

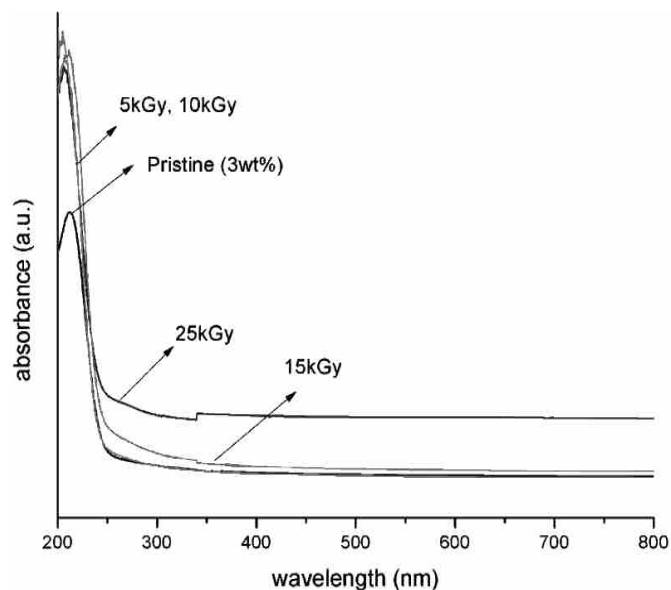


Fig.3. UV-Vis spectra of pristine and gamma irradiated PLGA nanocomposites samples containing 3wt% clay content

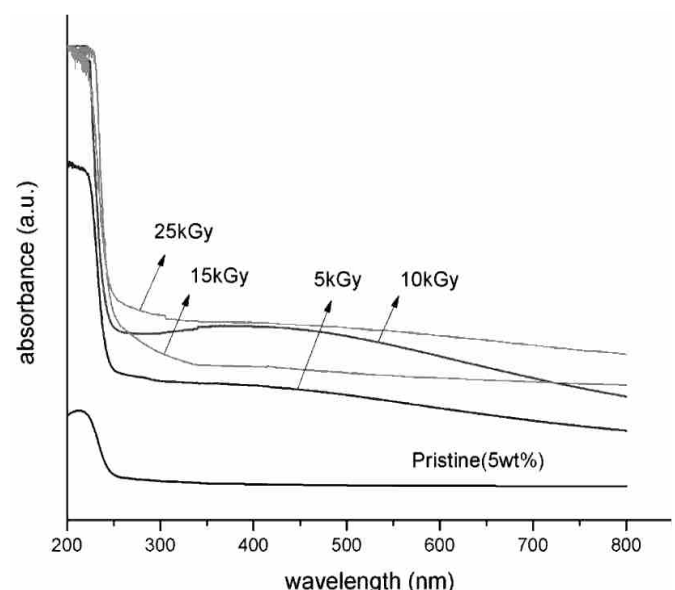


Fig.4. UV-Vis spectra of pristine and gamma irradiated PLGA nanocomposites samples containing 5wt% clay content

S.No.	Gamma dose (kGy)	(Band gap energy) sqrt(αE) (eV)	(Urbach's energy) ln(α) (eV)
1	Blank	4.81	0.22
2	5	4.7	0.23
3	10	4.62	0.48
4	15	4.8	0.36
5	25	4.84	0.3
6	50	4.92	0.21

Table 1. The variation of optical band gap energy and Urbach's energy with gamma dose in the pristine and gamma irradiated PLGA samples

Gamma Dose (kGy)	1wt%		3wt%		5wt%	
	Bandgap energy (eV)	Urbach energy (eV)	Bandgap energy (eV)	Urbach energy (eV)	Bandgap energy (eV)	Urbach energy (eV)
0	4.88	0.2	4.69	0.35	4.71	0.3
5	4.89	0.18	4.66	0.51	4.73	0.47
10	4.85	0.19	4.62	0.41	4.75	0.32
15	4.83	0.18	4.58	0.43	4.78	0.3
25	4.8	0.25	4.47	0.57	4.83	0.29

Table 2. The variation of optical band gap energy and Urbach's energy with gamma dose in the pristine and gamma irradiated PLGA/Cloisite® 30B nanocomposites samples

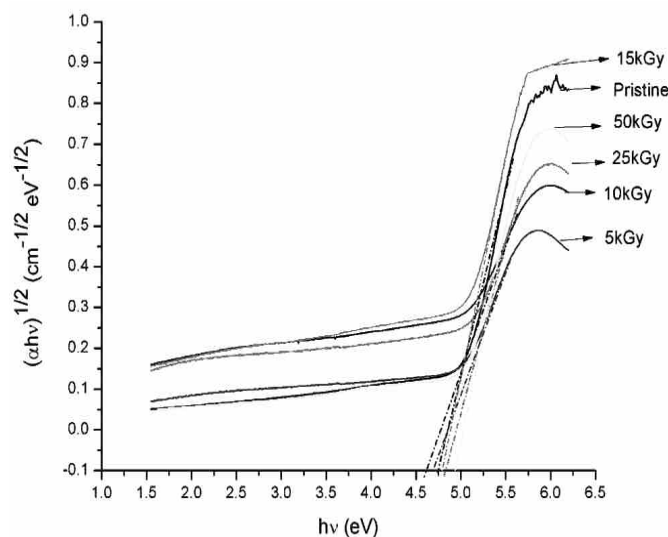


Fig.5. Extrapolation of Tuac's plot of the pristine and irradiated PLGA samples

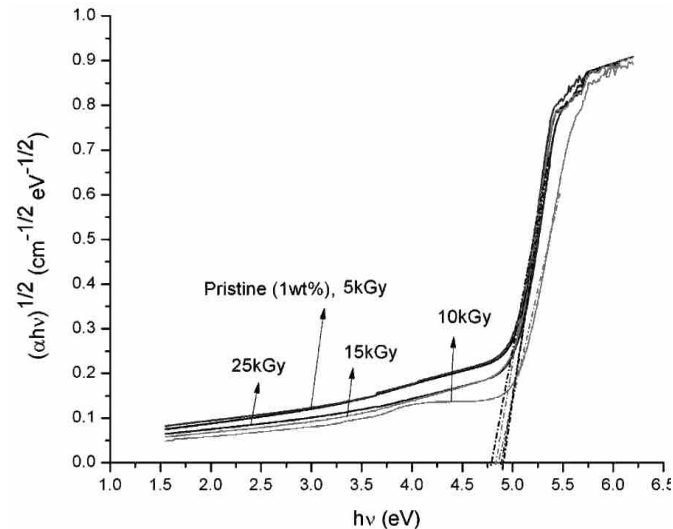


Fig.6. Extrapolation of Tuac's plot of the pristine and irradiated PLGA nanocomposites samples containing 1wt% clay content

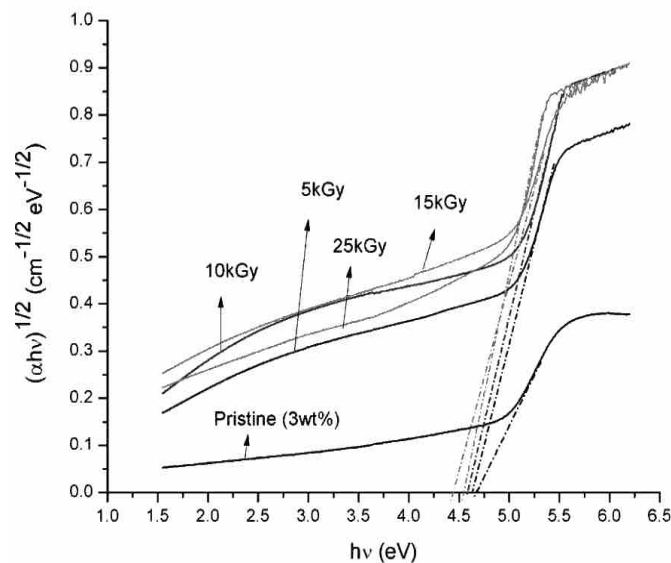


Fig.7. Extrapolation of Tuac's plot of the pristine and irradiated PLGA nanocomposites samples containing 3wt% clay content

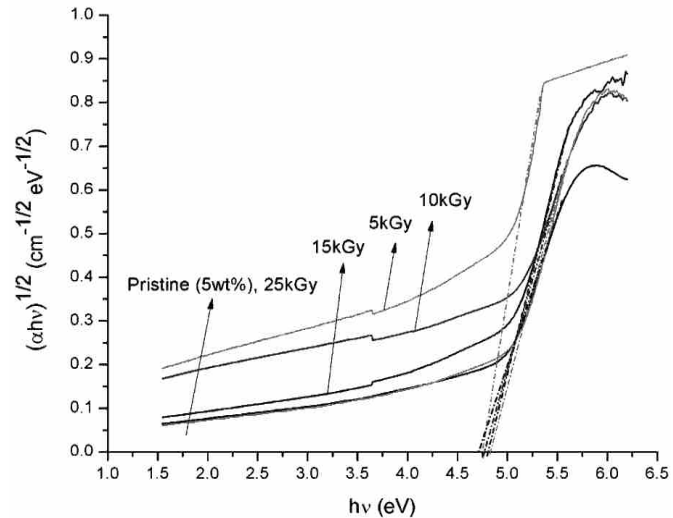


Fig.8. Extrapolation of Tuac's plot of the pristine and irradiated PLGA nanocomposites samples containing 5wt% clay content

It is also observed from Table 2, that there is a variation in band gap of PLGA nanocomposites with increasing dose of γ -radiation. With increasing dose rate, the values of the indirect band gap of nanocomposites samples containing 1wt% and 3wt% clay contents have been found to decrease however for 5wt% clay content the values are increasing (Table 2). The decrease in band gap in 1wt% and 3wt% nanocomposites samples indicates that random chain scission is not the primary mechanism. The decrease in band gap implies that due to impact of radiation treatment the nanocomposites samples containing small clay content got nicely distributed without any aggregation of *clay layers*. In case of 5wt% clay content, the band gap increases from 4.71 to 4.83 eV. This increase in band gap for 5wt% nanocomposites is probably due to the partial aggregation of clay layers in the polymer matrix as compared to nano level dispersion in 1wt% and 3wt% nanocomposites.

The irregularities in the band gap of the thin films or degree of structural disorder in amorphous materials was measured in terms of Urbach energy (E_u) and is determined from the inverse of the slope of the plots $\ln(\alpha)$ versus $h\nu$ [41-42]. The width of the band tails of the localized states are described by Urbach energy. The value of Urbach energy increases in 1wt% and 3wt% nanocomposite samples with increase in gamma dose but at 5wt%, E_u decreases with increase in fluence which may be due to recovery of irregularities in the band gap of polymer with crosslinking at high content of clay loading or decrease in the amorphicity of polymer.

3.2 FTIR analysis

The changes in chemical structure of neat PLGA and PLGA-based nanocomposites containing 1wt% and 5wt% of clay

content induced by gamma irradiation were determined using FTIR spectroscopy. FTIR spectrum of non-irradiated and irradiated PLGA samples at 5, 15, 25 and 50 kGy are shown in Fig. 9. The intensity of absorbed peak appeared at 1750 cm^{-1} in pristine and irradiated samples is related to carbonyl group of ester linkage. The relative intensity of this characteristic peak regularly decreases with radiation dose. This means that as a result of gamma irradiations, the radiation induced oxidation reaction of ester groups occur which leads to the formation of free radicals and inducing the formation of hydroxyl and carbonyl compounds [43]. The absorption band appearing in region $3400\text{--}3600\text{ cm}^{-1}$ is attributed to OH groups in alcohols or carboxylic acids. Upon irradiation with gamma dose, no significant changes have been observed. Similar results are deduced for the non-irradiated and irradiated nanocomposite samples at 5, 15 and 25kGy. FTIR spectra for PLGA/Clay nanocomposites containing 1wt% and 5wt % clay content are shown in Fig. 10 and Fig. 11 respectively. The comparison of the different FTIR spectra of pristine PLGA and irradiated nanocomposite samples reveals that there is shift of the band position of the irradiated nanocomposite samples in the presence of Cloisite[®] 30B in comparison with pristine PLGA. It is expected that the modifier will form hydrogen bond with epoxy in nanocomposites. It is observed from the spectra of Cloisite[®] 30B, Si–O bending bands (523 and 465 cm^{-1}) and the intensity of Si–O–Si stretching band (1048 cm^{-1}) is most sensitive to the degree of intercalation [44]. These bands are not observed in all SHI irradiated nanocomposites samples, indicating that the nanocomposites samples show exfoliated morphology.

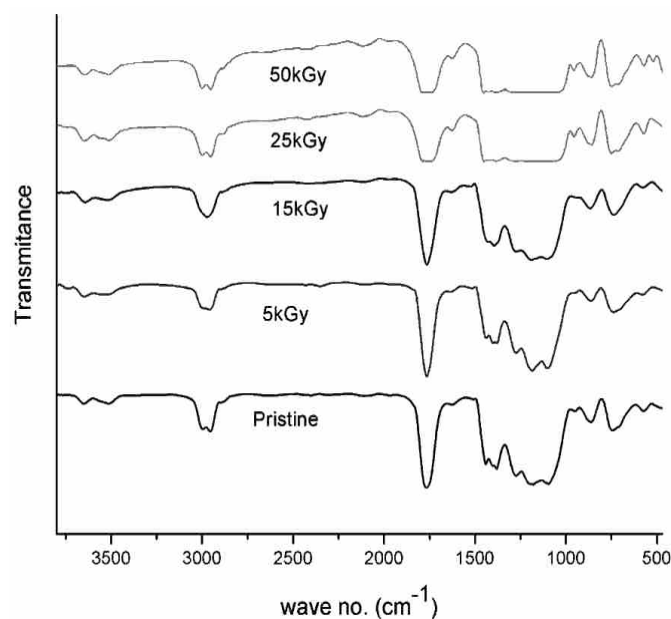


Fig.9. FTIR spectra of pristine and gamma irradiated PLGA samples

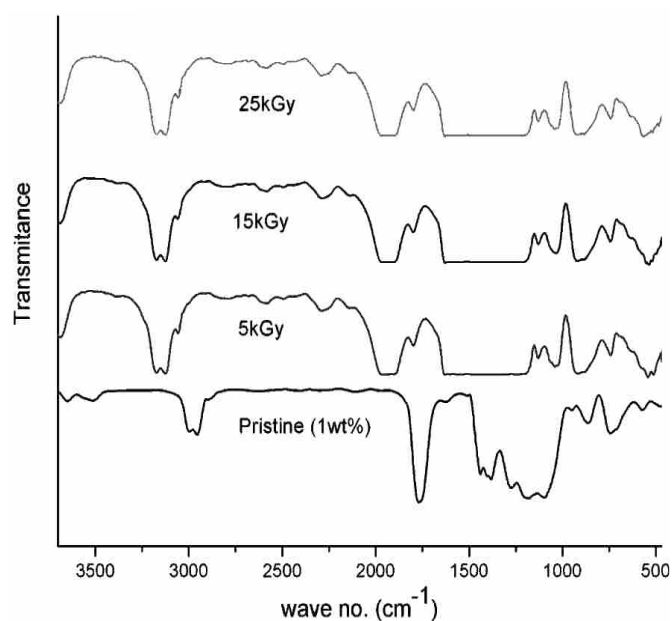


Fig.10. FTIR spectra of pristine and gamma irradiated PLGA nanocomposites samples containing 1wt% clay content at doses 5kGy, 15kGy and 25kGy

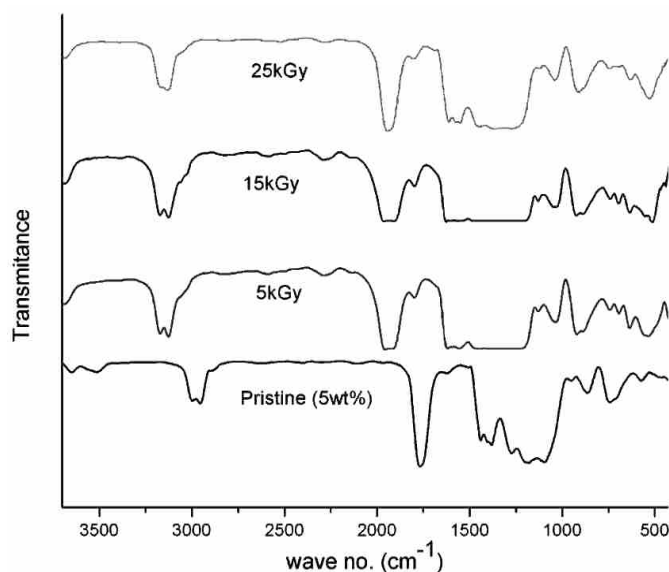


Fig.11. FTIR spectra of pristine and gamma irradiated PLGA nanocomposites samples containing 5wt% clay content at doses 5kGy, 15kGy and 25kGy

3.3 XRD analysis

XRD analysis was conducted on pristine and irradiated film samples to understand the effect of gamma dose on the structure of PLGA and PLGA/Clay nanocomposites. XRD spectrum of pristine and gamma irradiated PLGA samples does not show any crystalline peaks but a characteristic broad amorphous peak for all film samples as shown in Fig. 12. Amorphous materials will also diffract X-rays, but diffraction is much more diffuse, low frequency halo and peak of amorphous materials gives information about the statistical arrangement of atom in the neighbourhood of another atom [45-46]. As can be seen from

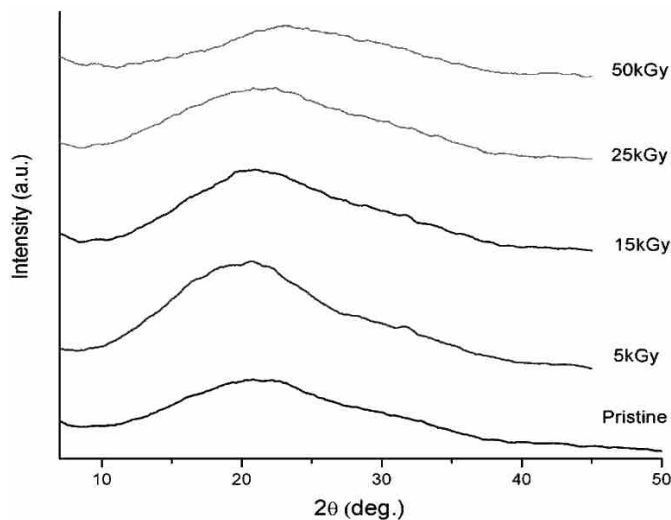


Fig.12. X- ray diffraction pattern for pristine and gamma irradiated PLGA samples

Fig. 12, absence of Bragg's diffraction peak but a broad hump appears at $2\theta \sim 21.35^\circ$ in the pristine PLGA sample, confirming the amorphous nature of the sample. The broadening of the diffraction peak was also observed in PLGA samples after irradiation. The reason of broadening of peak is the formation of defects after irradiation. Such defects, which may creates the new energy levels and leads to the broadening of peaks [47]. The irradiated samples also exhibit the same diffraction patterns except that peak shifts by a smaller angle. The shift in angular position and intensity change can be explained by change in lattice spacing [48]. The diffraction pattern of Cloisite® 30B displays a diffraction peak at $2\theta = 4.8$, corresponding to d_{001} (Fig. 13). The interlayer spacing is calculated from the d_{001} peak position using Bragg's law:

$$d_{00n} = n\lambda / 2(\sin \theta)$$

where n is an integer, θ is the angle of incidence of the X-ray beam, and $\lambda = 0.154$ nm is the X-ray wavelength. In Figs. 14 and 15, PLGA/Clay nanocomposites film samples with different loading of nanoclay i.e. 1wt% and 5wt%, after γ -irradiation have been observed. In the case of Cloisite® 30B based nanocomposites, the characteristic peak of irradiated samples does not show any d_{001} spacing. This may be due to extensive polymer penetration resulting in disruption of parallel stacking of the organoclay, causing in disordered and eventual delamination of the silicate layers in polymer matrix producing exfoliated morphology of nanocomposites, which consist of individual silicate layers dispersed in polymer matrix [49-50]. The XRD pattern of the PLGA shows a lack of intergallery clay diffraction due to complete exfoliation in pristine as well as those irradiated samples. This exfoliated structure is observed at all different Cloisite® 30B clay loadings and is in agreement with the FTIR data shown in Figs. 10 and 11.

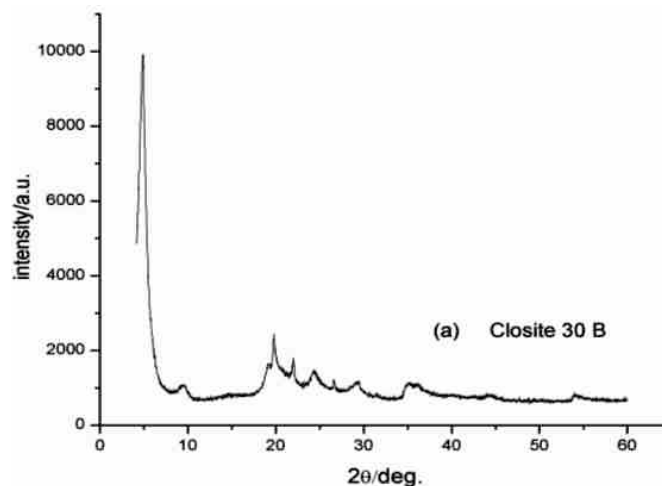


Fig.13. X-ray diffraction patterns of Cloisite® 30B

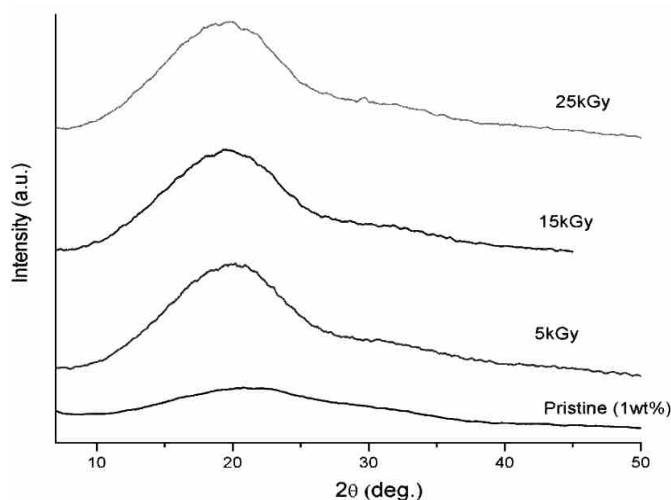


Fig.14. X- ray diffraction pattern for pristine and gamma irradiated PLGA nanocomposites samples containing 1wt% clay content at doses 5kGy, 15kGy and 25kGy

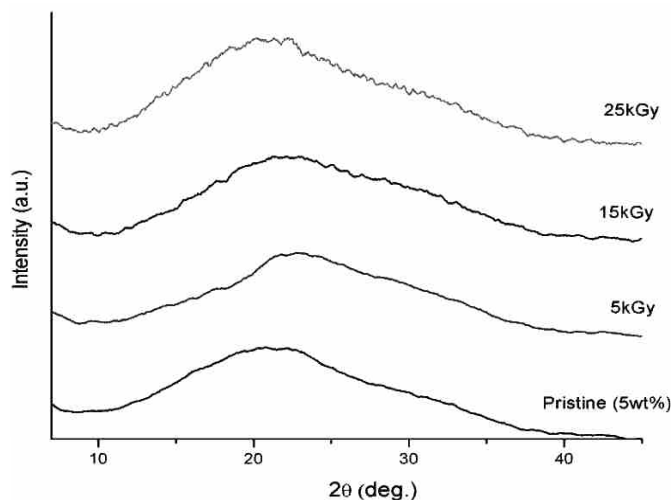


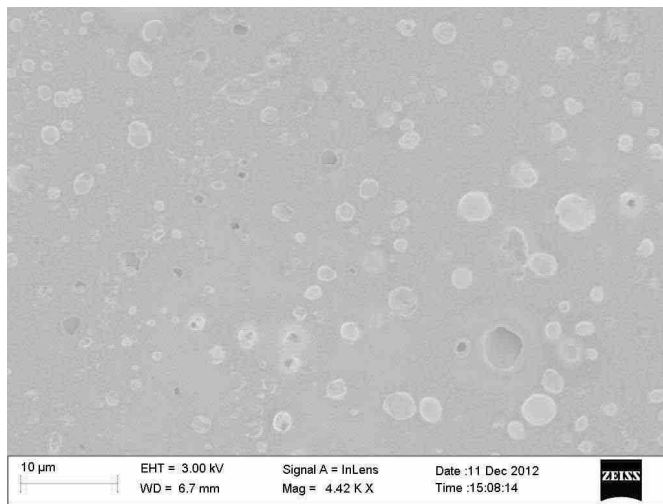
Fig.15. X- ray diffraction pattern for pristine and gamma irradiated PLGA nanocomposites samples containing 5wt% clay content at doses 5kGy, 15kGy and 25kGy

3.4 Morphological study

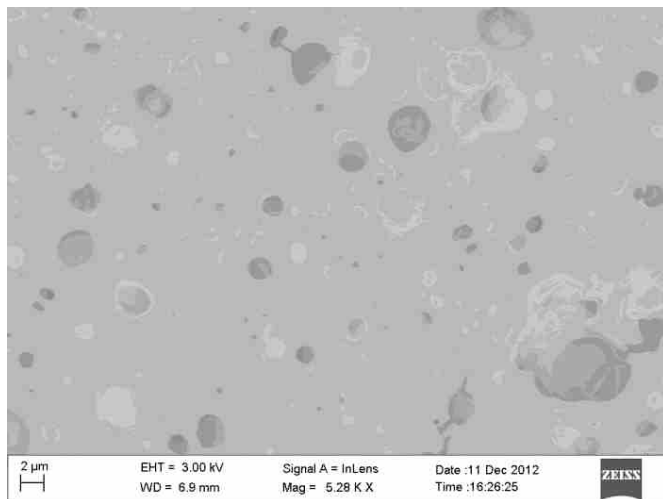
The morphological changes induced by γ -irradiation in the PLGA and PLGA/Clay nanocomposites samples are examined by SEM microscopy. Fig. 16(a-c) shows the SEM micrographs of the smooth surface of neat PLGA and fractured surfaces of PLGA samples after γ -irradiation. No significant defects are visible on the surface of neat PLGA samples but some small voids can be seen on the surface probably due to air pockets formed during preparation. These structures are present in both pristine PLGA as well as PLGA/Clay micrographs, thus, confirming that these are not clay agglomerations. The micrographs reveal also that no cracks are detected on the neat PLGA surface. At 50 kGy of gamma exposure, considerable defects are observed on the fractured surface of sample (Fig. 16(c)). These exposed samples have degraded, as evidenced by a rough surface, the appearance of microcavities of different sizes and shapes and the formation of cracks. The number and the size of the microcavities increase considerably with dose rate of gamma radiation. The chain scission of the ester bonds at high dose of γ -radiations could be responsible for defects at polymer surface.

Figures 17 and 18 exhibit the SEM micrographs of surfaces of PLGA/Clay nanocomposite before and after γ -irradiation. The SEM analyses reveal that significant changes in the morphology of PLGA/Clay nanocomposites have been induced by the γ -irradiation treatment in which higher level of dispersion is expected with the radiation dose. The effects are much less pronounced in the PLGA nanocomposite samples,

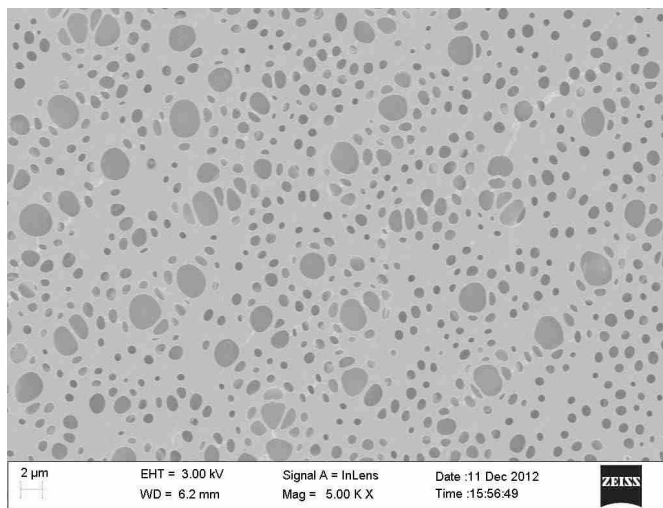
containing different clay content as compared to irradiated PLGA samples. In Fig. 18, the fractured surface of the PLGA nanocomposites containing 5wt% clay content exhibit a slightly rough surface before exposure, in which nanoparticles of Cloisite[®] 30B in the PLGA matrix are homogeneously dispersed. γ -irradiated PLGA nanocomposites film samples do not lead to significant degradation in contrast to previous observation for neat PLGA. With increasing irradiation dose, the orientation of silicate layers seems to be completely destroyed, and an exfoliated morphology occurs due to random distribution of clay layers into polymer matrix. The softening temperature of PLGA is quite low (40-60°C) and the temperature of the film samples during irradiation is expected to be much higher, this gives enough segmental or even translational energy to the polymer chains. As suggested by Lu et al. [51], free radicals and ions generated with high mobility upon irradiation, may diffuse in and/or out from the clay galleries. This rate of diffusion depends upon the irradiation dose rate, which may support the improvement of the steric interaction between clay layers and making exfoliated structure within the polymer [52]. The morphology of irradiated nanocomposites clearly indicates better dispersion of the clay particles of Cloisite[®] 30B in the PLGA matrix. The SEM observation also suggests that the PLGA/Clay nanocomposites containing different amounts of nanoclay have an exfoliated morphology, which is also in good agreement with the X-ray scattering patterns measurement.



(a)

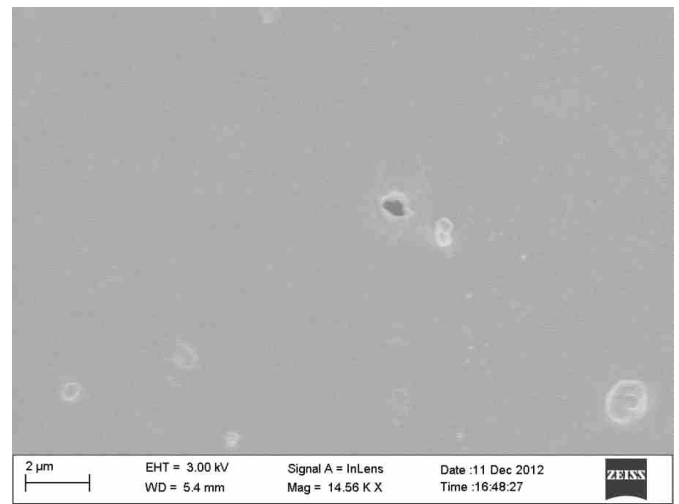


(b)

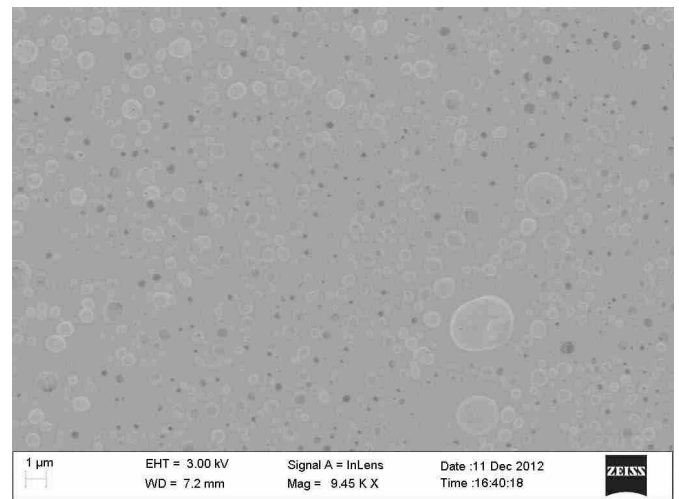


(c)

Fig.16. SEM micrographs of neat PLGA (a): Before irradiation and (b): After gamma irradiation of 25 kGy, (c) 50 kGy

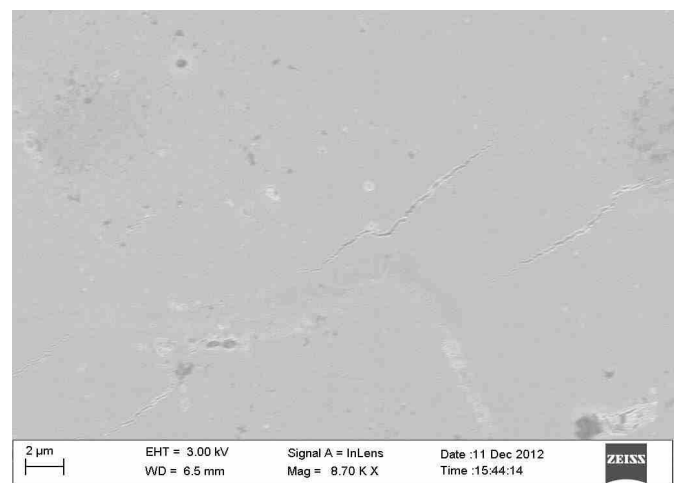


(a)

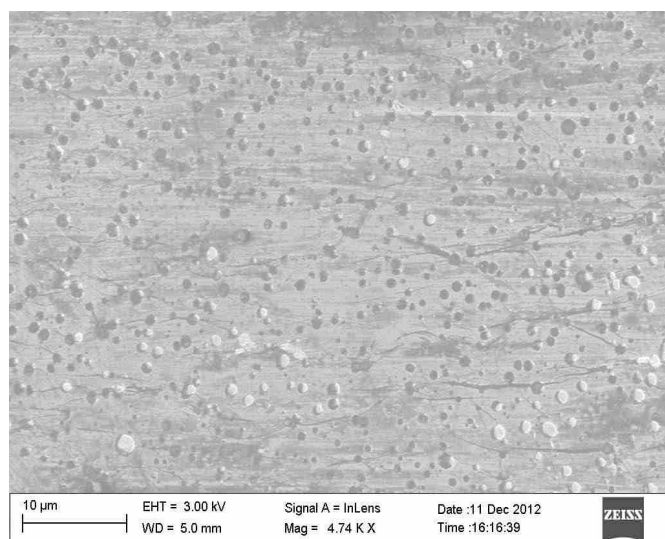


(b)

Fig.17. SEM micrographs of fractured surface for PLGA/Cloisite30B (1wt%) (a):Before irradiation and (b): After gamma irradiation of 25 kGy



(a)



(b)

Fig.18. SEM micrographs of fractured surface for PLGA/C30B (5wt%)
(a): Before irradiation and (b): After gamma irradiation of 25 kGy

4. CONCLUSION

The results reported in the present study show that PLGA and PLGA/Clay nanocomposites prepared by ultrasonication method and exposed to γ -irradiation exhibit significant changes in properties of the materials. The nature and extent of changes in morphology of irradiated nanocomposites are strongly affected by the presence of clay. Irradiation helps in a nano dispersion of clay layers in polymer matrix, and exhibiting exfoliated morphology especially at high dose. The remarkable changes are obtained in the optical properties which may be attributed to a formation of cross-linking/chain scission or recombination of the defects, which leads to an increase in the band gap energy. XRD and FTIR investigations also confirm the intermolecular interactions between clay and polymer chains after γ -radiations. The damage caused by γ -irradiation is found to be much more in PLGA samples as compared to irradiated PLGA nanocomposites. The present study of γ -irradiation of PLGA and PLGA/Clay nanocomposites has important implications for drug delivery and biomedical applications.

ACKNOWLEDGEMENT

The authors are thankful to IUAC, New Delhi for providing financial assistance and necessary facilities for accomplishment of the present work.

REFERENCES

- [1] Rychter P, Smigiel-Gac N, Pamuła E, Dmochowska A.M., Janeczek H, Prochwicz W, Dobrzy P. *2016 Materials* 2016, *64*, 1-17.
- [2] Parveen, S; Sahoo, S.K. Polymeric nanoparticles for cancer therapy. *J. Drug Targeting*. **2008**, *16*, 108-123.
- [3] Mohamed F, van der Walle CF. Engineering biodegradable polyester particles with specific drug targeting and drug release properties. *J. Pharm Sci.* **2008**, *97*, 71-87.
- [4] Raman, C; McHugh, A.J. A model for drug release from fast phase inverting injectable solutions. *J. Control Rel.* **2005**, *102*, 145-157.
- [5] Xie, J.W.; Tan, J.C.; Wang, C.H. Biodegradable films developed by electrospray deposition for sustained drug delivery. *J. Pharm Sci.* **2008**, *97*, 3109-3122.
- [6] Zhu G, Xu S, Wang J, Zhang L. Shape memory behaviour of radiation crosslinked PCL/PMVS blends. *Radiat Phys Chem.* **2006**, *75*, 443-448.
- [7] Miyajima, M; Koshika, A; Okada, J; Kusai, A; Ikida, M. The effects of drug physico-chemical properties on release from copoly (lactic/glycolic acid) matrix. *Int. J. Pharm.* **1998**, *169*, 255.
- [8] Lee, S.J.; Khang, G; Lee, Y.M; Lee, H.B. Interaction of human chondrocytes and NIH/3T3 fibroblasts on chloric acid-treated biodegradable polymer surfaces. *J. Biomater Sci. Polym Ed.* **2002**, *13*, 197-212.
- [9] Khang, G; Choi, M.K.; Rhee, J.M.; Lee, S.J.; Lee, H.B.; Iwasaki, Y; Nakabayashi, N; Ishihara, K. Biocompatibility of poly(MPC-co-EHMA)/poly(DL-lactide-coglycolide) blends. *Korea Polymer J.* **2001**, *9*, 107-115.
- [10] Khang, G; Lee, J.H.; Lee, I; Rhee, J.M.; Lee, H.B.; Interaction of different types of cells on poly(L-lactide-co-glycolide) surface with wettability chemo gradient. *Korea Polym J.* **2000**, *8*, 276-284.
- [11] Ray, S.S.; Maiti, P.; Okamoto, M.; Yamada, K; Ueda, K. New Poly(lactide)/Layered Silicate Nanocomposites- Preparation, Characterization, and Properties. *Macromolecules.* **2002**, *35*, 3104-3110
- [12] Delozier, D.M.; Orwoll, R.A.; Cahoon, J.F.; Johnston, N.J.; Smith, J.G.; Connel, J.W. Spatial Gradients in Particle Reinforced Polymers Characterized by X-ray. Attenuation and Laser Confocal Microscopy. *Polymer.* **2002**, *43*, 803-812.
- [13] Kim, D.W.; Blumstein, A.; Tripathy, S.K. Nanocomposite Films Derived From Exfoliated Functional Alumino silicate through Electrostatic Layer-by-Layer Assembly. *Chemistry of Materials.* **2001**, *13*, 1916-1922.
- [14] Fermeglia, M.; Ferrone, M.; Priet, S. Computer simulation of nylon-6/organoclay nanocomposites, prediction of the binding energy. *Fluid Phase Equilibria.* **2003**, *212*, 315-329.
- [15] Xie, L.; Lv, X.Y.; Han, Z.J.; Ci, J.H.; Fang, C.Q.; Ren, P.G. Preparation and performance of high-barrier low density polyethylene/organic montmorillonite nanocomposite. *Poly Plast Tech Eng.* **2012**, *51*, 1251-1257.
- [16] Kasirga, Y.; Oral, A.; Caner, C. Preparation and characterization of chitosan/ montmorillonite-K10 nanocomposites films for food packaging applications. *Polym Comp.* **2012**, *33*, 1874-1882.
- [17] Nugroho, P.; Mitomo, H.; Yoshii, F.; Kune, T. Degradation of poly(L-lactic acid) by γ -irradiation. *Polym Degrad Stab.* **2001**, *72*, 337-343.
- [18] Babanalbandi, A.; Hill, D.J.T.; O'Donnell, J.H.; Pomery, P.J.; Whittaker, A. An electron spin resonance study on γ -irradiated poly(L-lactic acid) and poly(D, L-lactic acid). *Polym Degrad Stab.* **1995**, *50*, 297-304.

- [19] Oliveira, L.M.; Araujo, E.S.; Guedes, S.M.L. Gamma irradiation effects on poly(hydroxybutyrate). *Polym Degrad Stab.* **2006**, *91*, 2157-2162.
- [20] Chu, C.C.; Zhang, L.; Coyne, L.D. Effect of gamma irradiation and irradiation temperature on hydrolytic degradation of synthetic absorbable sutures. *Journal of Applied Polymer Science.* **1995**, *56*, 1275-1294.
- [21] Alexis, F. Factors affecting the degradation and drug-release mechanism of poly(lactic acid) and poly[(lactic acid)-co-(glycolic acid)]. *Polym Int.* **2005**, *54*, 36-46.
- [22] Fawzy, Y.H.A.; Ali, A.E.H.; Maghraby, E.; Radwan, R.M. Gamma irradiation effect on the thermal stability, optical and electrical properties of acrylic acid/ methyl methacrylate copolymer films. *World J Cond Matt Phys.* **2011**, *1*, 12-18.
- [23] Nelson, J.F.; Standford, H.G.; Cutright, D.E. Evaluation and comparisons of biodegradable substances as osteogenic agents. *J Oral Surg.* **1997**, *3(6)*, 836-843.
- [24] Hollinger, J.O. Preliminary report on the osteogenic potential of a biodegradable copolymer of polylactide (PLA) and polyglycolide (PGA). *Biomed Mater Res.* **1983**, *17*, 71-82.
- [25] Kleinschmidt, J.; Marden, L.; Kent, D.; Quigley, N.; Hollinger, J. A multiphase system bone implant for regenerating the calvaria. *J Plast reconstr Surg.* **1993**, *91*, 581-588.
- [26] Levy, F.; Hollinger, J.; Szachowicz, E. Effect of a bioresorbable film on regeneration of cranial bone. *Plast Reconstr Surg.* **1994**, *93*, 307-311.
- [27] Zaidi, L.; Bruzard, S.; Kaci, M.; Bourmaud, A.; Gautier, N.; Grohens, Y. The effects of gamma irradiation on the morphology and properties of polylactide/Cloisite 30B nanocomposites. *Poly Degrad Stab.* **2013**, *98*, 348-355.
- [28] Touati, N.; Kaci, M.; Ahouari, H.; Bruzard, S.; Grohens, Y. The Effect of γ -Irradiation on the Structure and Properties of Poly(propylene)/Clay Nanocomposites. *Macromol Mater Eng.* **2007**, *292*, 1271-1279.
- [29] Suarez, J.C.M.; Mano, E.B.; Tavares, M.I.B. Tensile behaviour of irradiated recycled polyolefin plastics. *J. Appl Polym Sci.* **2000**, *78*, 899-909.
- [30] Hausberger, A.G.; Kenley, R.A.; DeLuca, P.P. Gamma Irradiation Effects on Molecular Weight and in Vitro Degradation of Poly(D,L-Lactide-CO-Glycolide) Microparticles. *Pharm Res.* **1995**, *12(6)*, 851-856.
- [31] Montanari, L.; Cilurzo, F.; Valvo, L.; Faucitano, A.; Buttafava, A.; Groppo, A.; Genta, I.; Conti, B. Gamma irradiation effects on stability of poly(lactide-co-glycolide) microspheres containing clonazepam. *J Control Release* **2001**, *75*, 317.
- [32] Montanari, L.; Costantini, M.; Signoretti, E.C.; Valvo, L.; Santucci, M.; Bartolomei, M.; Fattibene, P.; Onori, S.; Faucitano, A.; Conti, B.; Genta, I. Gamma irradiation effects on poly(dl-lactide-co-glycolide) microspheres. *J. Control. Release* **1998**, *56*, 219-229.
- [33] Zhang, L.; Ducharme, S.; Jiangyu, L. Microimprinting and ferroelectric properties of poly(vinylidene fluoride-trifluoroethylene) copolymer films. *Appl phys letter.* **2007**, *91*, 172906-172909.
- [34] Srivastava, A.K.; Virk, H.S. 50MeV lithium ion beam irradiation effects in poly vinylidene fluoride (PVDF) polymer. *Bull Mater Sci.* **2000**, *23*, 533-538.
- [35] Fink, D.R.; Klett, L.T.; Chadderton, J.; Cardoso, R.; Montiel, M.H.; Karanovich, V. Carbonaceous clusters in irradiated polymers as revealed by small angle X-ray scattering and ESR. *Nucl Instr Meth B.* **1996**, *111*, 303-314.
- [36] Zaki, M.F. Gamma-induced modification on optical band gap of CR-39 SSNTD. *J. Phys D Appl Phys.* **2008**, *4*, 175404.
- [37] Tauc, J. *Amorphous and Liquid Semiconductor.* Plenum, New York. **1974**.
- [38] Yang, Y.; Gao, Y.; Mei, X. Effects of gamma-irradiation on PLGA microspheres loaded with thienorphine. *Pharmazie.* **2011**, *66(9)*, 694-697.
- [39] Lee, J.S.; Chae, G.S.; Khang, G. The Effect of Gamma Irradiation on PLGA and Release Behavior of BCNU from PLGA Wafer. *Macromolecular Research.* **2003**, *11*, 352-356.
- [40] Kaur M, Singh S and Mehta R. **2014**, *Polymer Science, Ser. B, 56*, 657-663.
- [41] Mott, N.F.; Davis, E.A. *Electronic Processes in Non-Crystalline Materials*, second ed., Clarendon Press, Oxford. **1979**
- [42] Urbach, F. The long-wavelength edge of photographic sensitivity and of the electronic absorption of solids. *Phys Rev.* **1953**, *92*, 1324.
- [43] Zaidi, L.; Bruzard, S.; Kaci, M.; Bourmaud, A.; Nicolas Gautier, Yves Grohens, The effects of gamma irradiation on the morphology and properties of polylactide/Cloisite 30B nanocomposites. *Polym Degrad Stab.* **2013**, *98*, 348-355.
- [44] Mohamadi, S.; Sanjani, N.S. Studies on PEBAX/organoclay nanocomposites by melt-intercalation process, Effect of organoclay surface. *e-Polymers.* **2009**, *135*, 1-14.
- [45] Sperling, L.H. *An Introduction to Physical Polymer Science*, John Wiley and Sons, 3rd Ed. 2001.
- [46] Bradly, R.F. *Comprehensive Desk Reference of Polymer Characterization and Analysis*, American Chemical Society, Washington, D.C. **2003**
- [47] Kumar, V.; Sonkawade, R.G.; Dhaliwal, A.S. Gamma irradiation induced chemical and structural modifications in PM-355 polymeric nuclear track detector film. *Nucl Instr and Meth B.* **2012**, *290*, 59-63.
- [48] Kumar, R.; Prasad, R.; Vijay, Y.K.; Acharya, N.K.; Verma, K.C.; De, U. Ion beam modification of CR-39 (DOP) and polyamide nylon-6 polymers. *Nucl Instr and Meth B.* **2003**, *212*, 221-227.
- [49] Giannelis, EP, Krishnamoorti R, Manias E. Polymer-silicate nanocomposites, model system for confined polymers and polymer brushes. *Adv Polym Sci.* **1999**, *138*, 107-147.
- [50] Krikorian, V.; Pochan, D.J. Poly (l-Lactic Acid)/Layered Silicate Nanocomposite, Fabrication, Characterization, and Properties. *Chem Mater.* **2003**, *15*, 4317-4324.
- [51] Lu, H.; Hu, Y.; Xiao, J.; Kong, Q.; Chen, Z.; Fan, W. The influence of irradiation on morphology evolution and flammability properties of maleated polyethylene/clay nanocomposite. *Mater Lett.* **2005**, *59*, 648-651.
- [52] Koo, C.M.; Kim, M.J.; Choi, M.H.; Kim, S.O.; Chung, I.J. Mechanical and rheological properties of the maleated polypropylene-layered silicate nanocomposites with different morphology. *J Appl Polym Sci.* **2006**, *88*, 1526-1535.

